NASA/TM-2009-215708

# Flutter Sensitivity to Boundary Layer Thickness, Structural Damping, and Static Pressure Differential for a Shuttle Tile Overlay Repair Concept

*Robert C. Scott and Robert E. Bartels*
*Langley Research Center, Hampton, Virginia*

---

April 2009

# NASA STI Program . . . in Profile

Since its founding, NASA has been dedicated to the advancement of aeronautics and space science. The NASA scientific and technical information (STI) program plays a key part in helping NASA maintain this important role.

The NASA STI program operates under the auspices of the Agency Chief Information Officer. It collects, organizes, provides for archiving, and disseminates NASA's STI. The NASA STI program provides access to the NASA Aeronautics and Space Database and its public interface, the NASA Technical Report Server, thus providing one of the largest collections of aeronautical and space science STI in the world. Results are published in both non-NASA channels and by NASA in the NASA STI Report Series, which includes the following report types:

- TECHNICAL PUBLICATION. Reports of completed research or a major significant phase of research that present the results of NASA programs and include extensive data or theoretical analysis. Includes compilations of significant scientific and technical data and information deemed to be of continuing reference value. NASA counterpart of peer-reviewed formal professional papers, but having less stringent limitations on manuscript length and extent of graphic presentations.

- TECHNICAL MEMORANDUM. Scientific and technical findings that are preliminary or of specialized interest, e.g., quick release reports, working papers, and bibliographies that contain minimal annotation. Does not contain extensive analysis.

- CONTRACTOR REPORT. Scientific and technical findings by NASA-sponsored contractors and grantees.

- CONFERENCE PUBLICATION. Collected papers from scientific and technical conferences, symposia, seminars, or other meetings sponsored or co-sponsored by NASA.

- SPECIAL PUBLICATION. Scientific, technical, or historical information from NASA programs, projects, and missions, often concerned with subjects having substantial public interest.

- TECHNICAL TRANSLATION. English-language translations of foreign scientific and technical material pertinent to NASA's mission.

Specialized services also include creating custom thesauri, building customized databases, and organizing and publishing research results.

For more information about the NASA STI program, see the following:

- Access the NASA STI program home page at *http://www.sti.nasa.gov*

- E-mail your question via the Internet to help@sti.nasa.gov

- Fax your question to the NASA STI Help Desk at 443-757-5803

- Phone the NASA STI Help Desk at 443-757-5802

- Write to:
  NASA STI Help Desk
  NASA Center for AeroSpace Information
  7115 Standard Drive
  Hanover, MD 21076-1320

NASA/TM-2009-215708

# Flutter Sensitivity to Boundary Layer Thickness, Structural Damping, and Static Pressure Differential for a Shuttle Tile Overlay Repair Concept

*Robert C. Scott and Robert E. Bartels*
*Langley Research Center, Hampton, Virginia*

National Aeronautics and
Space Administration

Langley Research Center
Hampton, Virginia 23681-2199

April 2009

The use of trademarks or names of manufacturers in this report is for accurate reporting and does not constitute an official endorsement, either expressed or implied, of such products or manufacturers by the National Aeronautics and Space Administration.

Available from:

NASA Center for AeroSpace Information
7115 Standard Drive
Hanover, MD 21076-1320
443-757-5802

# Abstract

This paper examines the aeroelastic stability of an on-orbit installable Space Shuttle patch panel. CFD flutter solutions were obtained for thick and thin boundary layers at a free stream Mach number of 2.0 and several Mach numbers near sonic speed. The effect of structural damping on these flutter solutions was also examined, and the effect of structural nonlinearities associated with in-plane forces in the panel was considered on the worst case linear flutter solution. The results of the study indicated that adequate flutter margins exist for the panel at the Mach numbers examined. The addition of structural damping improved flutter margins as did the inclusion of nonlinear effects associated with a static pressure difference across the panel.

# Contents

**1 Introduction 3**

**2 Structural Model and Analysis 3**

**3 Aeroelastic Analyses for a Linear Structure 4**

3.1 Steady-State Analyses . . . 8

3.2 Aeroelastic Analyses, Zero Structural Damping . . . 8

3.3 Aeroelastic Analyses, Nonzero Structural Damping . . . 13

**4 Aeroelastic Analyses with Static Nonlinear Structural Effects 13**

4.1 Nonlinear Structural Analysis . . . 14

4.2 Static Aeroelastic Analysis With Nonlinear Structure . . . 15

4.3 Dynamic Aeroelastic Analysis with Nonlinear Structure . . . 16

**5 Concluding Remarks 21**

# 1 Introduction

An on-orbit installable Space Shuttle patch panel was developed at the NASA Johnson Space Center to be used in the event of damage to the thermal protection system tiles to enable safe re-entry. It consists of a thin flexible carbon fiber reinforced silicon carbide (C/SiC) plate backed with a layer of fibrous insulation that covers the area of damaged tile. The plate and underlying gasket are secured to the tile with auger-like fasteners through holes at discreet locations around the perimeter of the plate. As part of the development effort, a series of panel flutter analyses were performed to determine whether the concept met the required safety margins for the onset of flutter. These analyses indicated that at Mach numbers of 2.0 and higher, adequate panel flutter margins existed within the shuttle flight envelope. However, near Mach 1.0 empirical flutter analysis using the criteria described in reference 1 yielded inadequate flutter margins.

To address the concerns regarding flutter margins, flutter analyses were performed using CFL3D [2] where both inviscid (Euler) and viscous (Navier-Stokes) terms were used [3]. The inviscid analyses indicated that panel flutter onset would occur at lower dynamic pressures than had been predicted by the linear and empirical solutions; yet, the bottom line results were the same with sufficient flutter margin still remaining at Mach 2 and inadequate flutter margin when near Mach 1.0. The viscous flutter analysis for Mach 2.0 was consistent with the inviscid solution. The viscous flutter analyses near Mach 1.0 indicated that the flutter onset dynamic pressure when viscosity is included was, in fact, well outside the shuttle flight envelope. For this study, the free stream Mach number and boundary layers for the two Mach numbers examined were adjusted to roughly correspond to boundary layer profiles at body point 1800 calculated with OVERFLOW [4]. Body point 1800 is located on the lower surface at 80% of the vehicle length, on centerline.

The purpose of the present paper is to describe a follow-on study where the effects of boundary layer thickness were examined in a more general sense. Specifically, flutter solutions were obtained for thick and thin boundary layers at a free stream Mach number of 2.0 and several Mach numbers near sonic speed. In addition, the effects of structural damping were also considered as well as structural nonlinearities associated with in-plane forces in the panel.

# 2 Structural Model and Analysis

The overlay panel is constructed of a C/SiC composite material and is 15 inches wide by 25 inches long with a thickness of 0.04 inches. A series of holes is placed along the perimeter of the plate to accept the auger and washer fasteners that attach the overlay panel to Shuttle tile. For the structural analysis, material corresponding to the holes was not removed from the finite element model. The material properties used for the C/SiC material were taken from experimental data obtained for a 0.13-inch thick plate of similar construction [5]. C/SiC is a nonlinear material in the sense that the stress-strain curves for the material are linear only for small strain. Additionally, the stress-strain behavior is different for compressive and tensile loading. The linear structural analysis for vibration modes assumed an orthotropic material with a modulus that is the average of the moduli obtained from compression and tension tests at 2,000°F given in reference 5.

The NASTRAN [6] finite element model of the installed overlay plate is shown in Figure 1. The locations of the fasteners are indicated by the nodes where all degrees of freedom are constrained. The model consists of 26,529 nodes with a combination of CQUAD4 elements and CTRIA3 elements. The tile and gasket are not modeled and the structural damping is zero. An MSC.NASTRAN SOL 103, normal modes analysis was performed with the first 25 modes having frequencies between 64 and 670 Hz as shown in Table 1. Modes

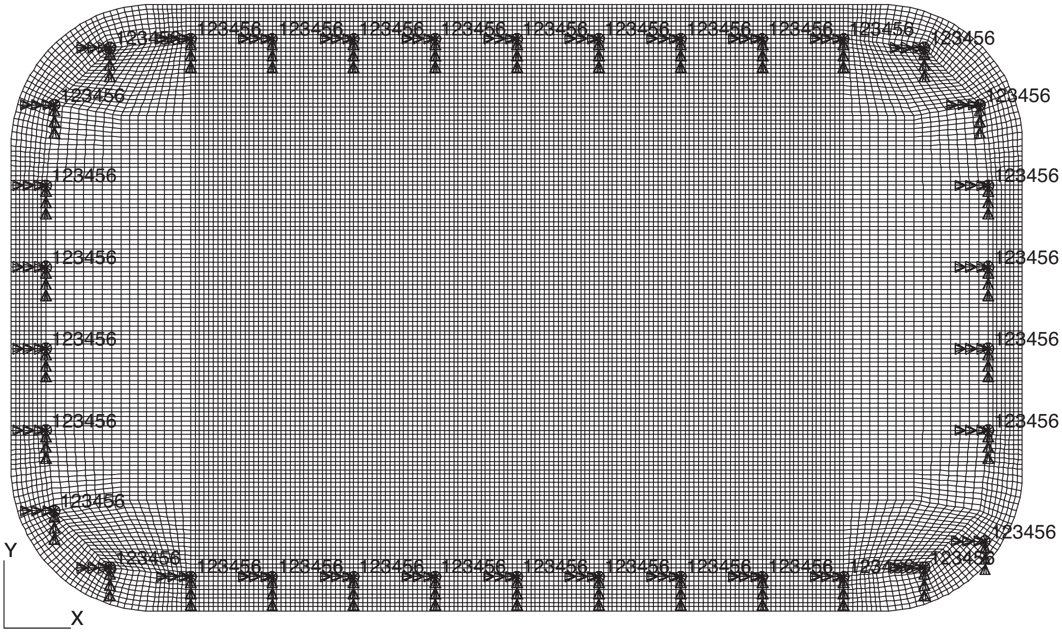

Figure 1. Installed overlay panel finite element mesh consisting of 26,529 nodes. The symbols and numbers on the mesh indicate the constrained degrees of freedom for the 34 nodes representing the fastener locations.

1 through 4 are shown in Figure 2. Additional details of the structural analysis including a mesh convergence study and comparison of free-vibration analysis with experimental data are described in reference [3].

## 3 Aeroelastic Analyses for a Linear Structure

The CFD code CFL3Dv6.4 [2, 7] was used for the flutter analysis. The CFL3D code solves the time-dependent conservation law form of the Reynolds-averaged Navier-Stokes equations using a finite-volume approach. Upwind-biasing is used for the convective and pressure terms while central differencing is used for the shear stress and heat transfer terms. Implicit time advancement is used with the ability to solve steady or unsteady flows. Sub-iteration and multigrid capabilities are available for improved accuracy and convergence acceleration.

The typical procedure for CFL3D flutter analysis is to initially obtain a static aeroelastic solution prior to running a solution to determine dynamic stability [7]. The static solution is obtained by using artificially large values of damping ratio in the analysis, and CFL3D is run until in it converges, establishing the static aeroelastic solution and associated flow field. Next, the dynamic analysis is performed. The damping ratio is set to a realistic value and the generalized coordinates are given small initial velocities. The analysis is run until dynamic aeroelastic stability can be established: if the generalized coordinate values converge to a finite value then the system is stable; but if they grow with time, then the system is unstable. For each free-stream flow condition of interest, flutter onset is determined by varying the dynamic pressure until the system becomes unstable.

Free stream temperature, velocity, and density (used in the dynamic pressure calculation) were interpolated based on Mach number from the ISSHVFW Shuttle trajectory. Reynolds numbers were estimated using standard atmosphere properties [8] for the interpolated altitude associated with the target Mach numbers. Note that for steady (non-aeroelastic)

Table 1. Modal frequencies from NASTRAN SOL 103, normal modes analysis.

| Mode | Frequency rad/sec | Frequency Hz |
|---|---|---|
| 1 | 405.4 | 64.5 |
| 2 | 580.5 | 92.4 |
| 3 | 886.8 | 141.1 |
| 4 | 1044.6 | 166.2 |
| 5 | 1212.5 | 193.0 |
| 6 | 1318.8 | 209.9 |
| 7 | 1502.8 | 239.2 |
| 8 | 1871.0 | 297.8 |
| 9 | 1918.8 | 305.4 |
| 10 | 2023.1 | 322.0 |
| 11 | 2192.4 | 348.9 |
| 12 | 2457.7 | 391.2 |
| 13 | 2480.6 | 394.8 |
| 14 | 2539.8 | 404.2 |
| 15 | 2889.4 | 459.9 |
| 16 | 3117.0 | 496.1 |
| 17 | 3320.7 | 528.5 |
| 18 | 3333.2 | 530.5 |
| 19 | 3420.4 | 544.4 |
| 20 | 3505.6 | 557.9 |
| 21 | 3793.5 | 603.8 |
| 22 | 3890.9 | 619.3 |
| 23 | 4067.8 | 647.4 |
| 24 | 4201.6 | 668.7 |
| 25 | 4215.0 | 670.8 |

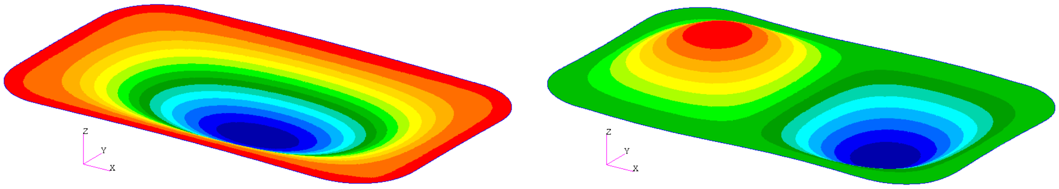

(a) Normal mode 1. (b) Normal mode 2.

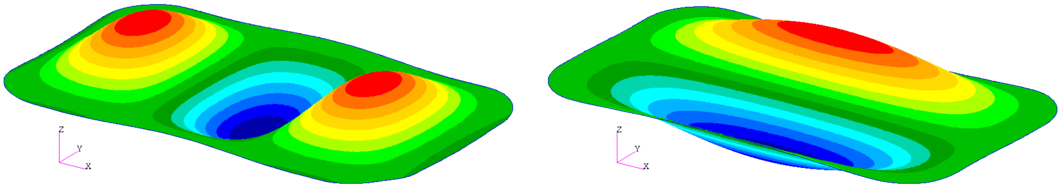

(c) Normal mode 3. (d) Normal mode 4.

Figure 2. Vertical displacement of the first four normal modes of overlay panel obtained using NASTRAN SOL 103. For each mode, red indicates maximum z values and blue represents minimum z values.

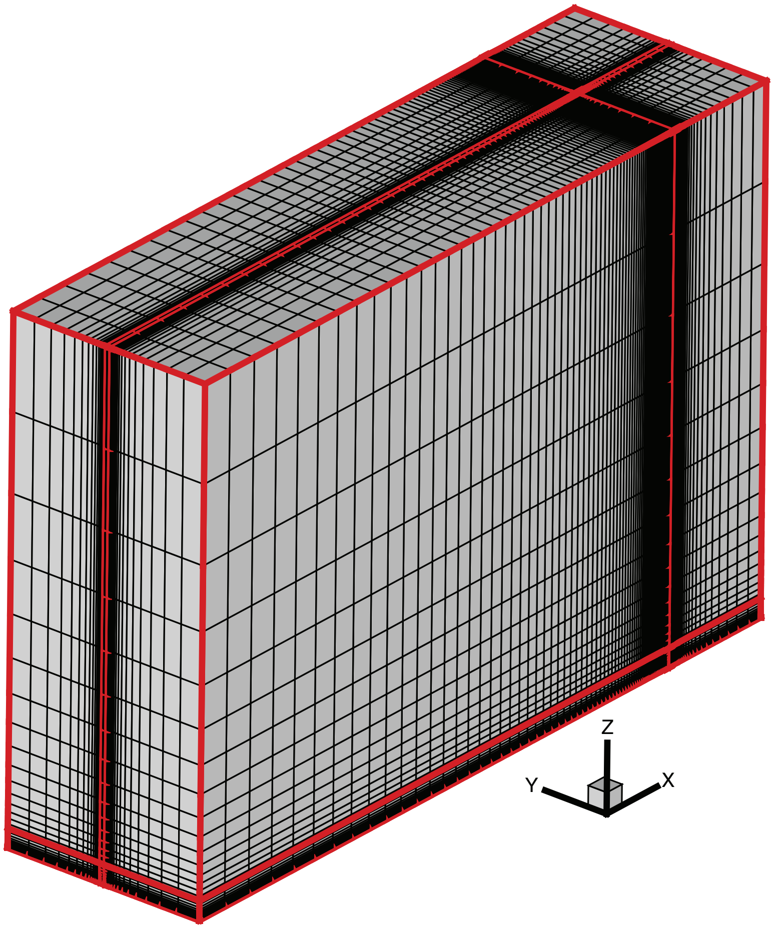

Figure 3. Computational grid used in viscous panel flutter analysis. Red lines denote block boundaries.

analyses, only free stream Mach number, Reynolds number, and temperature are required. Aeroelastic analyses require the selection of a velocity and dynamic pressure.

In the previous study [3] two separate computational grids were generated for the two free stream Mach numbers considered. These meshes extended the upstream boundary of the plate by 415 and 860 inches, respectively. The intent of that study was to match the boundary layer profile from an OVERFLOW analysis of the shuttle at body point 1800. For this study, a new, single computational grid was used, and the boundary conditions were adjusted to control boundary layer thickness. For the thick boundary layer, the no-slip boundary condition started 803.26 inches upstream of the panel, and for the thin boundary layer, the no-slip boundary condition started 35.15 inches upstream of the panel.

Figure 3 shows the volume grid used in the analysis where the computational grid dimensions in the x, y and z directions are 249, 97, and 65, respectively. To run these jobs on multiprocessor systems, the grid was split into 24 blocks whose boundaries are denoted by the red lines, and the block index dimensions along with the boundary conditions were selected to be multigridable to at least two coarser levels. Figure 4 shows the entire surface grid, as well as a close-up of the surface grid in the vicinity of the overlay plate. The upstream boundary of the grid is x=-1,264.8 inches and the downstream boundary is x=256.81 inches. The lateral limits are y=-207.2 and y=220.2, and the vertical limit is z=1,036.21

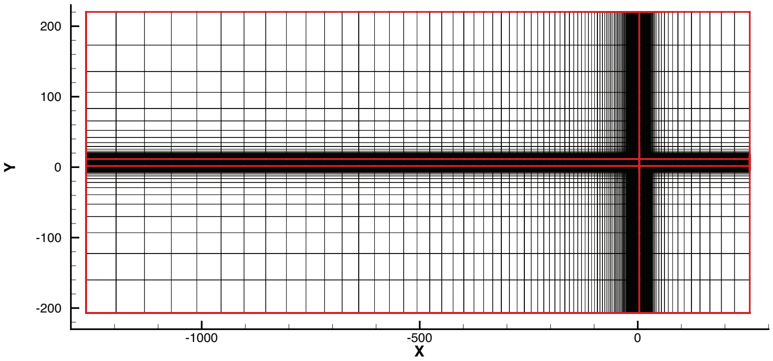
200
100
Y
0
-100
-200
-1000
-500
0
X

(a) Surface grid, red lines denote block boundaries.

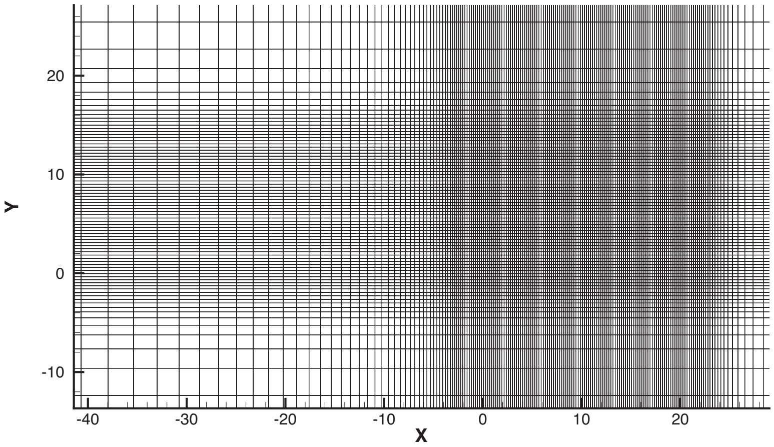
20
10
Y
0
-10
-40
-30
-20
-10
0
10
20
X

(b) Surface grid, overlay plate region.

Figure 4. Surface grid used in viscous panel flutter analysis.

inches. Note that in this computational space, the overlay panel occupies the space between -2.44 inches and 25.56 inches in the x-direction and -0.97 and 14.03 inches in the y-direction.

## 3.1 Steady-State Analyses

The first step in an aeroelastic analysis is to obtain a converged steady-state solution where the structure is treated as rigid. For these solutions, local time stepping was employed with a CFL number of 2.0. In all cases multigrid was used with two coarser meshes and the finest mesh, described above. The Spalart-Allmaras turbulence model was used in each analysis. The steady-state solutions were deemed sufficiently converged for the purposes of the subsequent aeroelastic analysis when the residual had been reduced by at least 4.5 orders of magnitude. Ten steady-state solutions were obtained using the Mach numbers, Reynolds numbers, and temperatures interpolated from the ISSHVFW Shuttle trajectory and the boundary conditions associated with the thick and thin boundary layer solutions. For these ten steady-state solutions, the y+ values at the first grid point off the surface ranged from between 0.54 and 1.34.

The local Mach numbers at the centerline, leading edge of the overlay plate are shown in Figure 5 for the thin and thick boundary layer cases. The thin boundary layers are on the order of 2 inches thick and should be representative of a point near the leading edge of the vehicle. The thin boundary layers contain about 35 grid points. The thick boundary layers are on the order of 10 to 15 inches thick and should be representative of a point well downstream of a wing leading edge or nose of the orbiter. Finally, it is observed that the Mach 0.98 and 1.02 solutions yield nearly identical flow in the vicinity of the panel. As such, the Mach 1.02 solution was not considered in the aeroelastic analyses.

## 3.2 Aeroelastic Analyses, Zero Structural Damping

Static and dynamic aeroelastic analyses are performed using an appropriate steady-state solution as the starting point. For aeroelastic analysis, additional input parameters are required in the input deck. These parameters include the free stream velocity and dynamic pressure, as well as, the modal frequencies noted in Table 1. In addition, a file containing the mode shape displacements for the computational surface mesh must also reside in the CFL3D working directory.

In the present study, the method described in reference 9 was employed for generating the CFL3D modal input file (aesurf.dat). The codes based on this paper calculate a spline interpolation of the NASTRAN mode shapes (.f06 file) to the surface mesh shown show in Figure 2. Figure 6 shows the computational mesh displacements associated with normal modes 1 and 2. Here, it is evident that the modal displacements in the computational mesh were extrapolated to a rectangular shape defined by the maximum length and width of the plate instead of having the rounded corners of the original NASTRAN model. This approximation was necessary because of a limitation in the code of reference 9, but it should have minimal effect on the solution. Due to limited resources available for this study, the thickness of the plate (0.04 inches) was not modeled in the computational mesh. Finally, it should be pointed out that when modal displacements are displayed they are greatly exaggerated from the actual physical displacements. The edge displacements shown in the figure are physically meaningful, but the actual displacements are quite small, generally much less than 10% of the panel thickness.

The general procedure was to perform a sequence of two CFL3D runs. The first, a static aeroelastic run, used a damping ratio for all modes of 0.999 and zero initial modal displacements and velocities. After 400 time steps, the static aeroelastic solution was sufficiently converged, and a second, dynamic, CFLD3D run was performed using the restart file from the first. For this dynamic run, structural damping is set to zero and and the initial modal

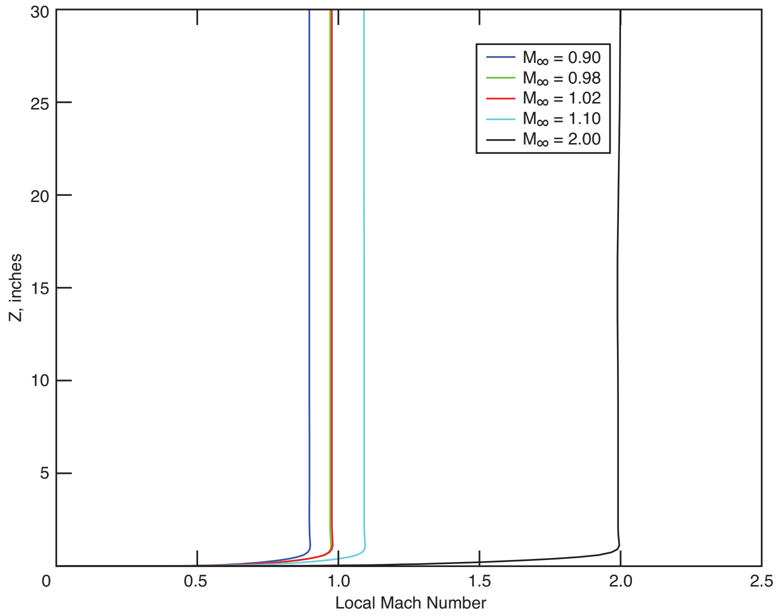

(a) Thin Boundary Layer

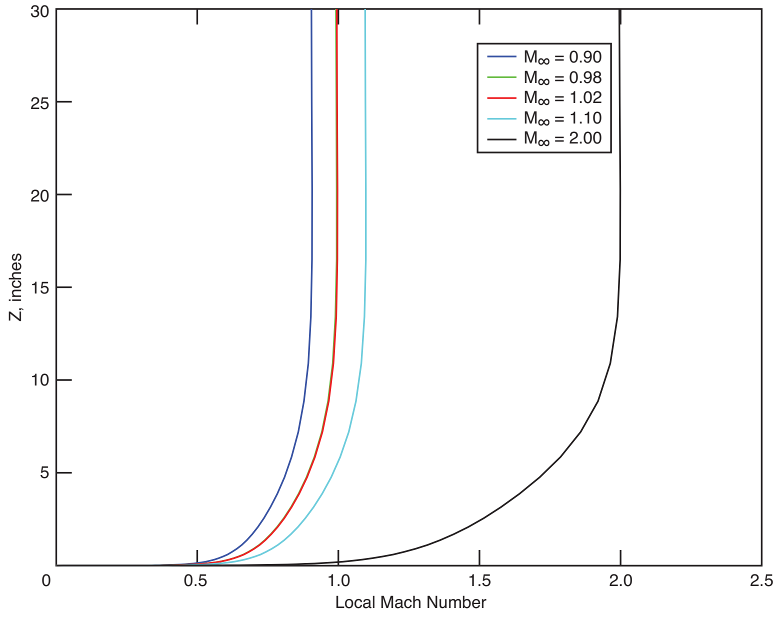

(b) Thick Boundary Layer

Figure 5. Boundary layers at overlay panel leading edge calculated using CFL3D.

velocities are given nonzero values. Dynamic aeroelastic stability is determined by observing whether the modal amplitudes grow or decay with time. Figure 7 shows the generalized coordinate time histories of the first four modes for stable and unstable values of dynamic pressure. The data shown to the left of the vertical line represents the static aeroelastic run where a large damping value is used. The data to the right of the vertical bar is obtained from a subsequent analysis where damping is set to zero and the generalized coordinates are give a small initial velocity.

The strategy for determining flutter onset that was employed in this study was to vary free stream dynamic pressure while holding all other input parameters constant. Essentially, this amounts to varying the free stream density. Strictly speaking, the flutter solutions obtained in this way aren't matched point solutions. However, for the purposes of assessing flutter margins, this approach was deemed adequate. By varying free stream dynamic pressure and examining the generalized coordinate time histories like those shown in Figure 7, the stability characteristics for the thick and thin boundary layer cases were obtained. Exact values of flutter onset dynamic pressure were not obtained as this is relatively time consuming and would provide little value added to the objectives of this study. Instead, the flutter onset dynamic pressure was shown to reside in a relatively narrow range of free stream dynamic pressure.

The zero damping ratio flutter results are shown in Table 2. Examination of these data indicate that the effect of boundary layer thickness is most pronounced near sonic speeds. Thicker boundary layers had a stabilizing effect on the plate at Mach numbers 1.10 and 0.98. At supersonic and subsonic Mach numbers, the thick and thin boundary layers yielded similar flutter dynamic pressures. Significant flutter margins in dynamic pressures were obtained for all conditions except the Mach 1.1, thin boundary layer case. Here the flutter margin in dynamic pressure is a little over 2.0.

Table 2. Summary of flutter onset range of normalized dynamic pressure ($q/q_\infty^{nominal}$).

| $M_\infty$ | Thick BL | | Thin BL | |
|---|---|---|---|---|
| | Stable | Unstable | Stable | Unstable |
| 2.00 | 4.5 | 5.0 | 4.5 | 5.0 |
| 1.10 | 6.0 | 6.5 | 2.0 | 2.5 |
| 0.98 | 5.5 | 6.0 | 3.5 | 4.0 |
| 0.90 | 4.0 | 4.5 | 4.0 | 4.5 |

In Table 3 the results of the present study are compared with those from reference 3. Here, dimensional dynamic pressure is shown for cases where comparable results were previously generated. In the previous study, the viscous flutter onset value was obtained with a boundary layer that is similar, but not identical to the thick boundary layer used here. The two studies are quite consistent with each other with regard to general trends and actual flutter onset dynamic pressures. Both studies show an insensitivity to boundary layer thickness at supersonic Mach numbers. This is indicated by the fact that the Mach 2.0 flutter dynamic pressure ranges are the same for the thick and thin boundary layers, and similarly for the Mach 1.75 analyses from reference 3, the fluter onset values are nearly identical for the viscous and inviscid cases. For Mach 1.1, the thick boundary layer result is very consistent with the previous viscous flutter onset value. For the Mach 1.1 thin boundary layer analysis, a significant drop in flutter dynamic pressure is noted as compared with the thick boundary layer case. This trend is consistent with the previous study where the inviscid flutter onset value was much lower than its viscous counterpart.

Before proceeding with additional aeroelastic analysis, a few words about the actual physical displacement of the overlay panel is warranted. When working with a modal rep-

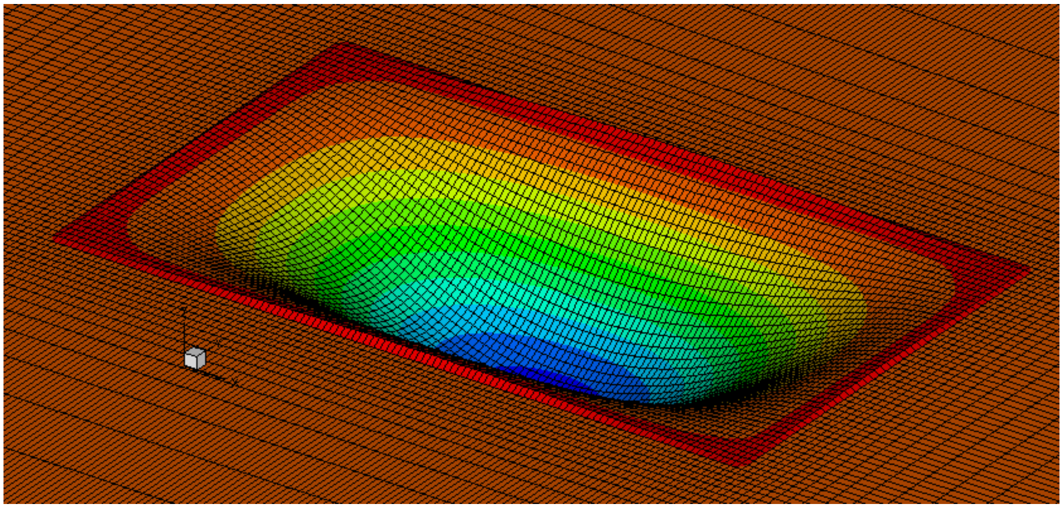

(a) Mode 1.

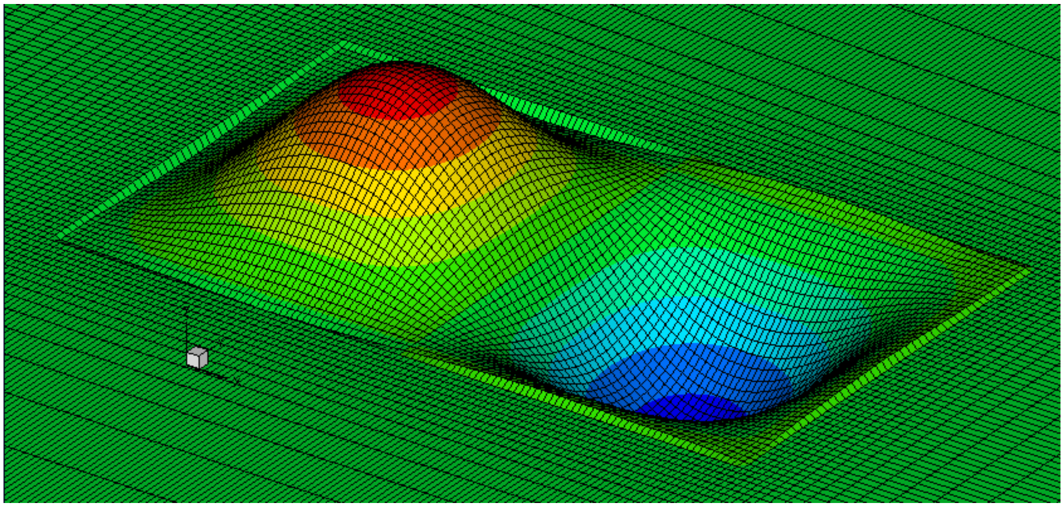

(b) Mode 2.

Figure 6. Normal modes 1 and 2 interpolated to the CFD surface grid. For each mode, red indicates maximum z values and blue represents minimum z values.

Table 3. Comparison of dynamic pressures (psf) with those from reference 3.

| $M_\infty$ | Present Study | | | | Previous Study (Flutter Onset) | | |
|---|---|---|---|---|---|---|---|
| | Thick BL | | Thin BL | | CFL3D | | Piston Theory* |
| | Stable | Unstable | Stable | Unstable | Viscous | Inviscid | or Empirical** |
| 2.00 | 1,177 | 1,307 | 1,177 | 1,307 | | | 1,352* |
| 1.75 | | | | | 850 | 890 | |
| 1.10 | 1,083 | 1,173 | 361 | 451 | 1,050 | 275 | 375** |

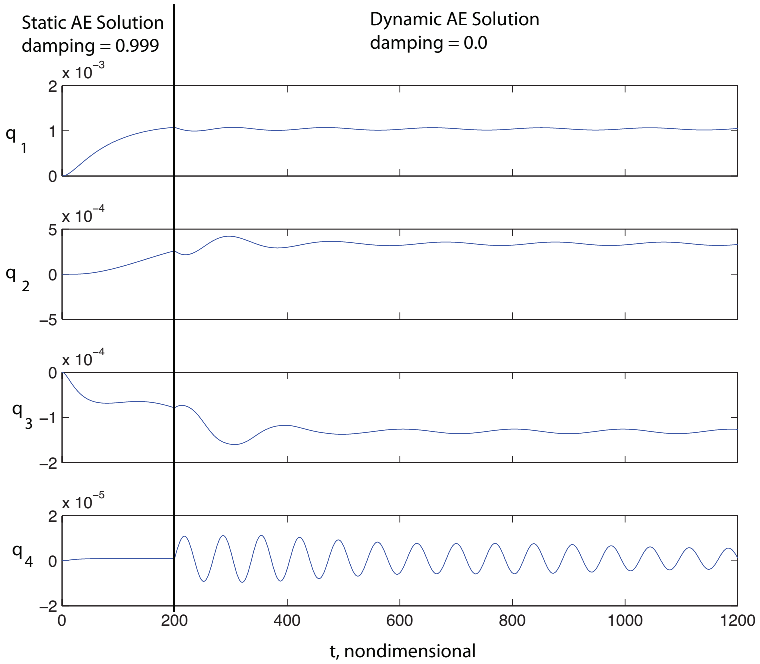

(a) $q_\infty = 2.0 q_\infty^{nominal}$.

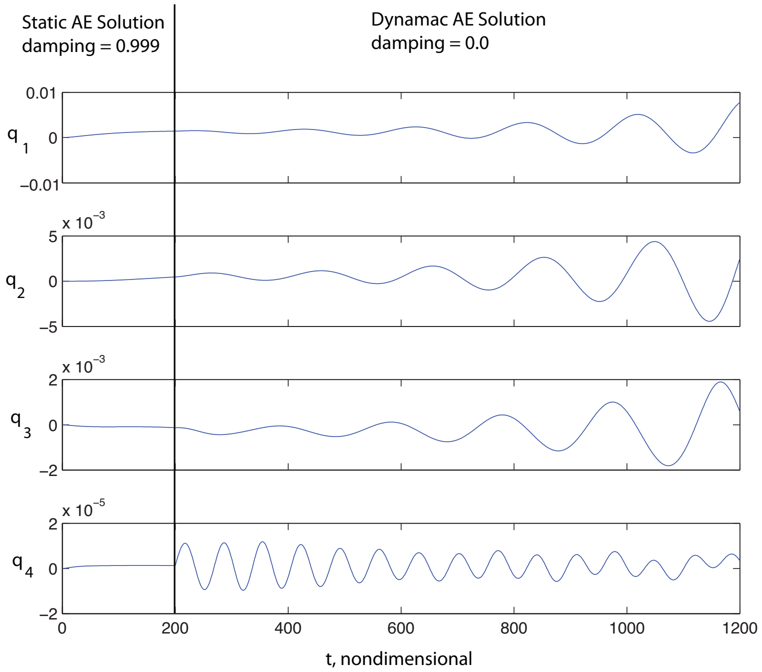

(b) $q_\infty = 2.5 q_\infty^{nominal}$.

Figure 7. Generalized coordinate time histories for Mach 1.10, thin boundary layer, for stable and unstable values of dynamic pressure. Flutter frequency = 68 Hz.

resentation of a structure, the net displacement of any point on that structure is a sum of the generalized coordinates times their respective mode shape displacement at that point. In the case of panel flutter, the static and dynamic displacement is governed largely by the first few modes especially modes 1 and 2. For the panel examined here, the maximum, normalized modal displacement is approximately 48 and 46, respectively for modes 1 and 2. Thus, the maximum panel displacement can be approximated by the summation the generalized coordinates for modes 1 and 2 times these modal displacements. Examination of the static aeroelastic solutions associated with the nominal dynamic pressures yields a maximum static panel displacement of approximately 0.05 inches. For the elevated values of dynamic pressure where flutter was obtained, maximum static panel deflections of up to 0.5 inches were obtained. The dynamic component for aeroelastically stable analyses was generally on the order of 0.05 inches or less. For the unstable cases where the amplitudes were diverging, the dynamic component was a function of the length of the simulation. In all dynamic analyses, any nonlinearities in the aerodynamics were fully captured, but structural nonlinearities were not. Panel flutter tends to result in a limit cycle due to structural nonlinearities, but this feature can not be captured in the analyses contained herein.

### 3.3 Aeroelastic Analyses, Nonzero Structural Damping

The procedure for this analysis is exactly the same as previously described except that the CFL3D analysis where stability is determined is run with nonzero values for damping ratio. The strategy employed here was to take the unstable dynamic pressure for each case in Table 2 and examine what value of damping is necessary to yield a stable or neutrally stable result. The results shown in Table 4 indicate a general trend where lower Mach number cases are more sensitive to damping than higher Mach number cases. The low Mach number cases were stabilized by a relatively modest, 2% damping. The supersonic cases in three out of four cases, were not stabilized by the addition of 10% damping. It should be pointed out that since the exact flutter onset values are not known, it is unclear how far from neutral stability these unstable cases were. Thus, the trend noted above remains tentative. Nonetheless, these analyses have shown that structural damping does have a stabilizing effect on flutter and provides some guidance on the level of damping required to have an effect.

Table 4. Structural damping effects on panel stability.

| $M_\infty$ | Thick BL | | | Thin BL | | |
|---|---|---|---|---|---|---|
| | $q/q_\infty^{nominal}$ | damping | Stability | $q/q_\infty^{nominal}$ | damping | Stability |
| 2.00 | 5.0 | 0.10 | unstable | 5.0 | 0.10 | unstable |
| 1.10 | 6.5 | 0.05 | stable | 2.5 | 0.10 | unstable |
| 0.98 | 6.0 | 0.02 | neutral/stable | 4.0 | 0.02 | neutral/stable |
| 0.90 | 4.5 | 0.02 | stable | 4.5 | 0.02 | stable |

## 4 Aeroelastic Analyses with Static Nonlinear Structural Effects

For panel structures, in-plane tension forces are stiffening terms, and if the tension forces are constant, a linear problem results. However, when out-of-plane forces are applied to a panel that is restrained at its edges, the tension and, as a result, the stiffness are both functions of the out-of-plane deformation. This results in a nonlinear problem. In this section of the

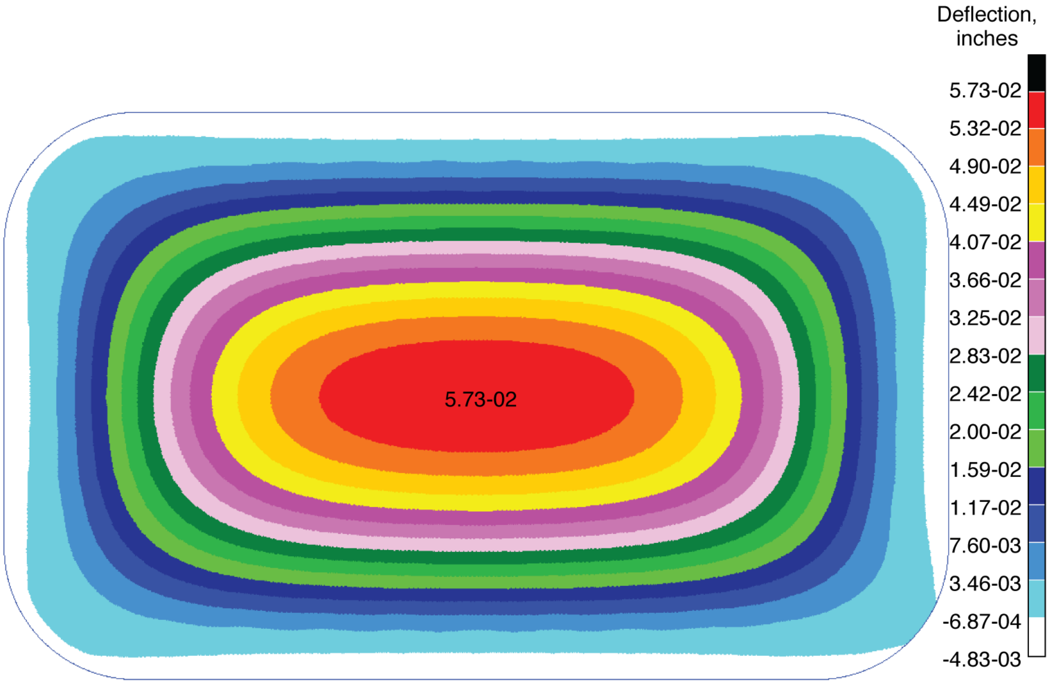

Figure 8. Overlay panel deflection due to a static pressure difference across the panel of 0.1 psi obtained using NASTRAN SOL 106.

paper, the static effects of the out-of-plane pressure forces and deformations on the Shuttle overlay panel will be considered for the previously examined Mach 1.10, thin boundary layer case. This was the case that showed the lowest flutter margin and was thus selected for this assessment. It should also be pointed out that only positive pressure differences were considered where the panel was deformed outward. Negative values would tend to suck the panel against the shuttles tiles and hole filler material making the panel unlikely to flutter, or at the very least, require a fully nonlinear flutter analysis that is far beyond the scope of the present study.

The following subsections will describe and demonstrate the various elements of the aeroelastic analysis with static nonlinear effects. First, NASTRAN will be used to show the effects of static pressure difference on the natural frequencies of the overlay panel. Next, a procedure that loosely couples NASTRAN and CFL3D to obtain a static aeroelastic solution will be shown. Finally, a method for utilizing the preceding analysis procedures for dynamic aeroelastic analysis will be shown and demonstrated for the Mach 1.10, thin boundary layer case.

## 4.1 Nonlinear Structural Analysis

This type of static nonlinear problem can be solved using NASTRAN SOL 106. This solution procedure essentially performs a series of linear analyses where the load is incrementally increased to the desired level. As these iterations proceed, the stiffness matrix is updated to include the stiffening effects of in-plane tension. This process is repeated within NASTRAN until the solution converges. Figure 8 shows the results of a static nonlinear analysis where the static pressure difference across the panel is 0.1 psi.

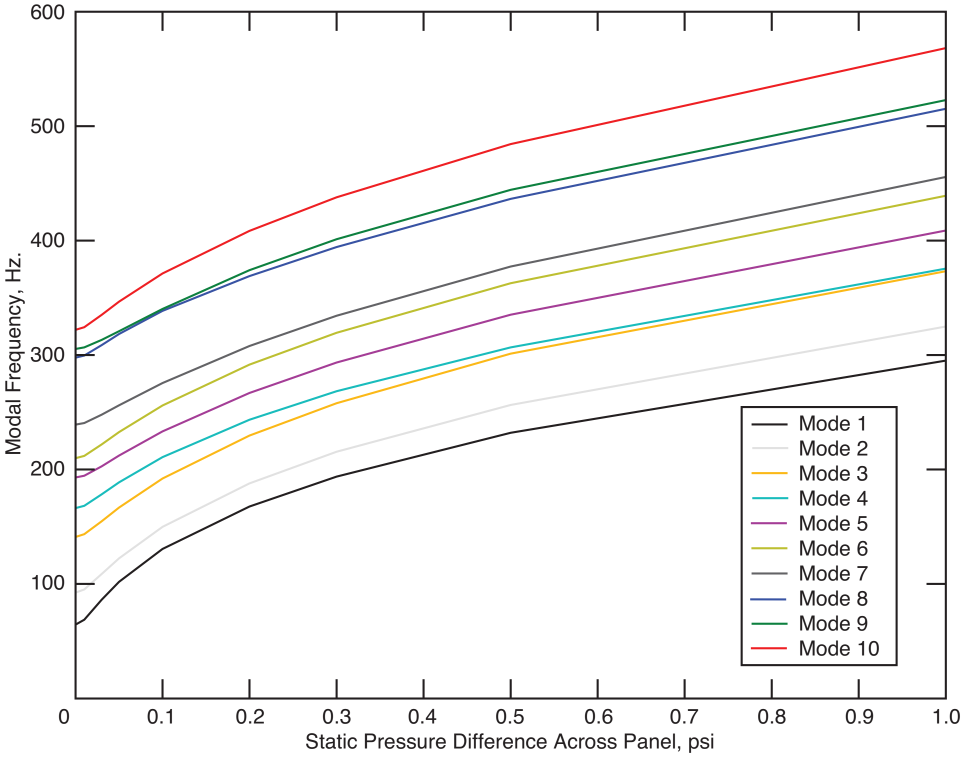

Figure 9. Natural frequency variation with static pressure difference across panel.

Using the method described in reference 10, a linear normal modes analysis (NASTRAN SOL 103) can be performed using the stiffness matrices from the converged NASTRAN SOL 106 analysis. Figure 9 shows how the frequencies of the first 10 normal modes vary as a result of performing sequential NASTRAN SOL 106 and 103 analyses for each static pressure difference. For the overlay panel, the modal frequencies are strong functions of the static pressure difference across the panel.

For the purposes of this study, a static pressure difference of 0.1 psi was arbitrarily assumed for the subsequent static and dynamic aeroelastic analysis. While this specific value was arbitrary, the decision was guided by the fact that a negative value would tend to suck the panel in against the tiles surrounding the hole or hole filler material both of which should be stabilizing effects. Also, the positive value of 0.1 psi was deemed large enough to provide a meaningful increase in modal frequencies as indicated in Figure 9. For this pressure, the frequency of the first mode doubles, and the frequency of the tenth mode increases by 15%.

## 4.2 Static Aeroelastic Analysis With Nonlinear Structure

Reference 11 describes a procedure to loosely couple CFL3D with NASTRAN for the purpose of obtaining a static aeroelastic solution that includes membrane type structural nonlinearities. This procedure was developed for a 2-D problem and was enhanced for the present 3-D problem. The goal of this procedures is to take the output of one code and make it available to the other. In this case, MATLAB [12] scripts (m-files) were written to do the following: 1) Read and pass the pressure coefficient data from the CFL3D output to the input of the NASTRAN SOL 106 analysis; and 2) Process and pass the NASTRAN structural analysis results (nodal displacements) to CFL3D. The details of these two procedures will be described next.

To transfer pressures from CFL3D to NASTRAN, the pressure coefficients were read from a CFL3D output file (cfl3d.prout). These coefficients were converted to pressures using the dynamic pressure appropriate for the Mach number and altitude being examined, and the resulting pressures were then interpolated to the structural mesh using linear interpolation. Finally, a bulk data file (.bdf) containing PLOAD2 cards is generated. This pressure data file is used in the NASTRAN SOL 106 analysis by way of an include statement in the main input deck.

To transfer the structural displacements from NASTRAN to CFL3D, the displacements are read from the NASTRAN output file (.f06). The structural displacements are then interpolated to the CFD grid points and written to the file newsurf.p3d. Within the CFL3D input file, the keyword idef_ss is set to unity which forces CFL3D to read the newsurf.p3d file and deform the grid accordingly. Due to an apparent bug in CFL3D where the surface deformation defined in newsurf.p3d is added at each time step, two CFL3D runs are required here. First, CFL3D is run for a single time step with key word idef_ss=1 so that volume grid is deformed in to the static aeroelastic shape defined by the file newsurf.p3d. Then CFL3D is restarted and run with idef_ss=0 for multiple time steps sufficient for the generalized forces to converge. To improve convergence, CFL3D is run in steady mode (iunst=0) for this analysis.

To conduct a static aeroelastic analysis, these two procedures are repeated until convergence. For the case of 0.1 psi pressure difference, a converged static aeroelastic solution is shown in Figure 10. As the problem is dominated by the static pressure difference, only three cycles were necessary for convergence with a cycle defined as a converged CFL3D analysis followed by a converged SOL 106 structural analysis. For this panel, the SOL106 analysis required about twice the CPU time as a SOL 103 analysis. This deflection can be compared with the non static aeroelastic analysis shown in Figure 8. Unlike the displacements in Figure 8, the displacements in Figure 10 are not symmetric from left to right.

## 4.3 Dynamic Aeroelastic Analysis with Nonlinear Structure

Several previously described analysis procedures will now be combined to perform the overlay panel flutter analysis that includes static nonlinear structural effects. These procedures include the nonlinear static aeroelastic analysis where NASTRAN SOL 106 is coupled with CFL3D followed by a NASTRAN normal modes analysis using the stiffness matrix from a prior nonlinear analysis. The previously described normal mode interpolation to the CFL3D surface grid along with the conventional modal flutter analysis within CFL3D will also be used. The modal flutter analysis procedure has many steps that can most easily be described in the following list.

1. Obtain a converged, nonlinear static aeroelastic solution using the loosely coupled NASTRAN SOL 106 and CFL3D static solution procedure.

2. Perform a NASTRAN SOL 103 analysis (normal modes analysis), using the final stiffness matrix from the preceding step.

3. Extract the frequencies and mode shapes from the NASTRAN SOL 103 output file. Put modal frequencies in CFL3D input file.

4. From the converged static aeroelastic solution in step 1, restart CFL3D (irestart=1) from previous steady run in unsteady mode (iunst=2) with modal deflection turned off (moddfl=-1).

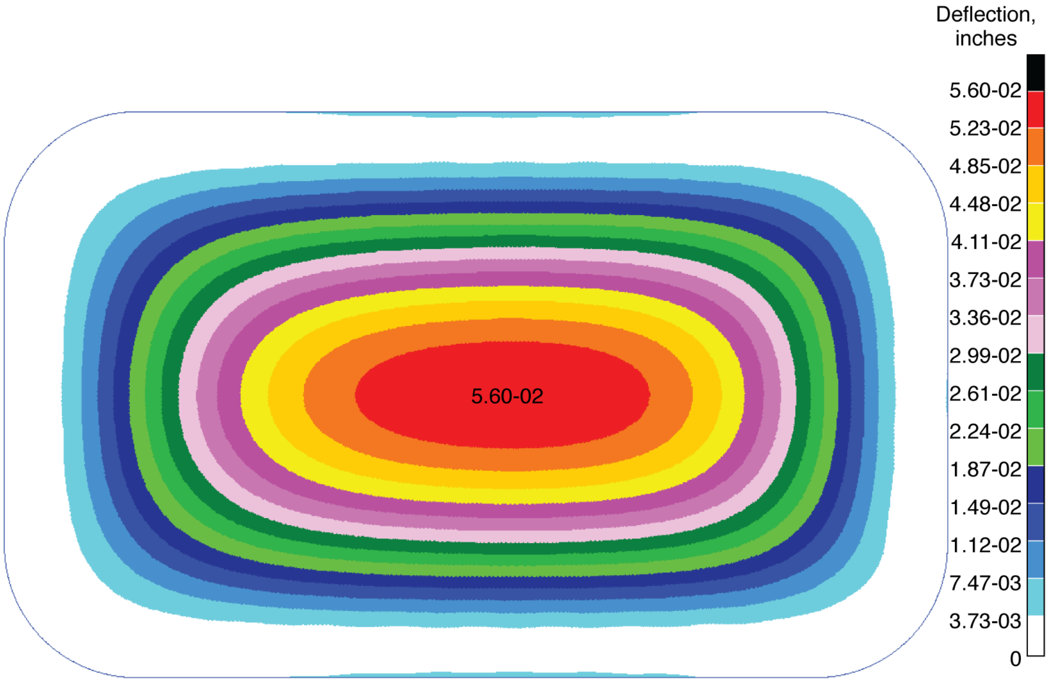

Figure 10. Overlay panel deflection from nonlinear static aeroelastic solution with pressure differential across the panel of 0.1 psi, the thin boundary layer, and Mach 1.10.

5. Extract converged generalized forces from the CFL3D output, put these values in the CFL3D input file as input parameter gf0. This step ensures that the pressure forces and internal stresses initially sum to zero so that no additional static aeroelastic deformation is obtained within CFL3D.
6. Restart CFL3D (irestart=1) with modal deformation turned off (moddfl=-1). After this run, net generalized forces should be near zero. Without this step, a transient in the generalized force will be introduced.
7. Restart CFL3D (irestart=1) with modal deformation turned on (moddfl=0) and a large value of modal damping (damp=0.999). This will remove any generalized coordinate transient associated with the net generalized force not being identically zero.
8. Restart CFL3D (irestart=1) with modal deformation turned on (moddfl=0) , modal damping set to zero (damp=0.0), and a perturbation value for the modal velocities (x0(2*n)=0.05). This step in the procedure is where stability is determined.

For the Mach 1.10, thin boundary layer case with static pressure difference of 0.1 psi, Figure 11 compares the first two normal modes obtained from step 2, above, with those obtained from the linear procedure used previously in this paper. The nonlinear static procedure has a significant effect on both mode shapes as shown here, as well as, the modal frequencies as previously shown in Figure 9. Both of these effects can be expected to alter the flutter behavior of the panel.

For the Mach 1.10, thin boundary layer case with static pressure difference of 0.1 psi and $q_\infty = 5.5 q_\infty^{nominal}$, the generalized force and generalized coordinate time histories associated with steps 4, 6, 7, and 8 are shown in Figure 12. The vertical lines separate the steps which

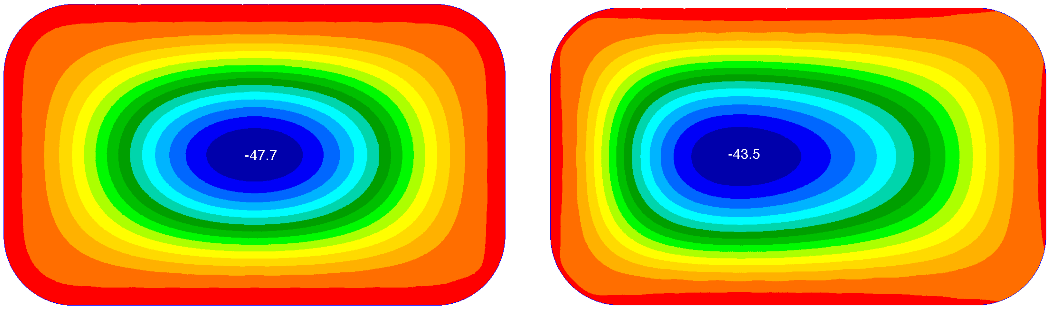

(a) Mode 1, Nominal Procedure.

(b) Mode 1, Nonlinear Static Procedure.

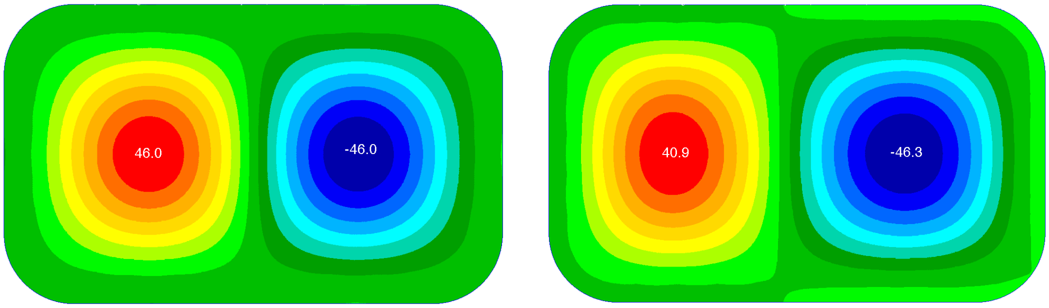

(c) Mode 2, Nominal Procedure.

(d) Mode 2, Nonlinear Static Procedure.

Figure 11. Comparison of the first two mode shapes obtained using only NASTRAN SOL 103 with mode shapes obtained using the modified procedure where NASTRAN SOL 103 is proceeded by the nonlinear, static aeroelastic solution (NASTRAN SOL 106 coupled with CFL3D). For each mode, red indicates maximum z values and blue represents minimum z values.

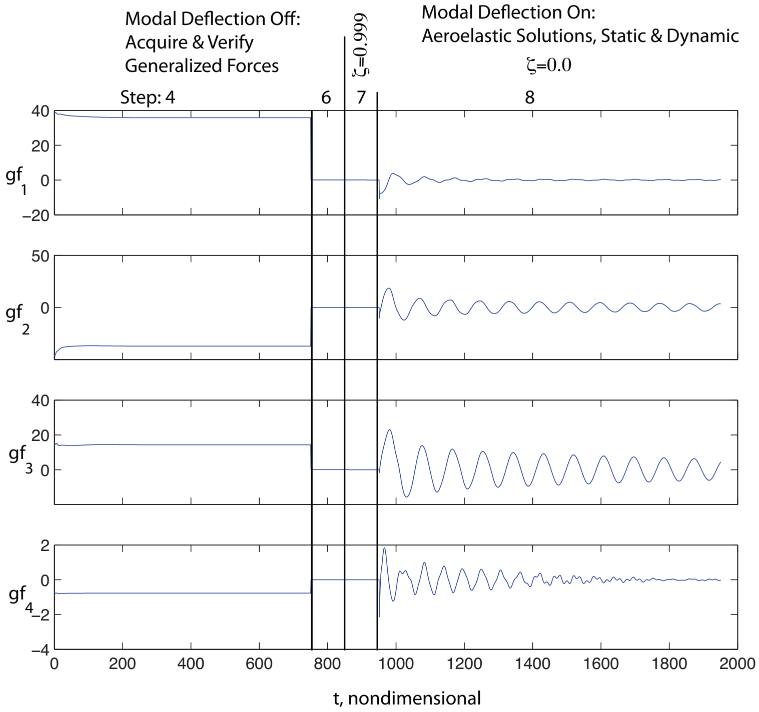

(a) Generalized force time histories.

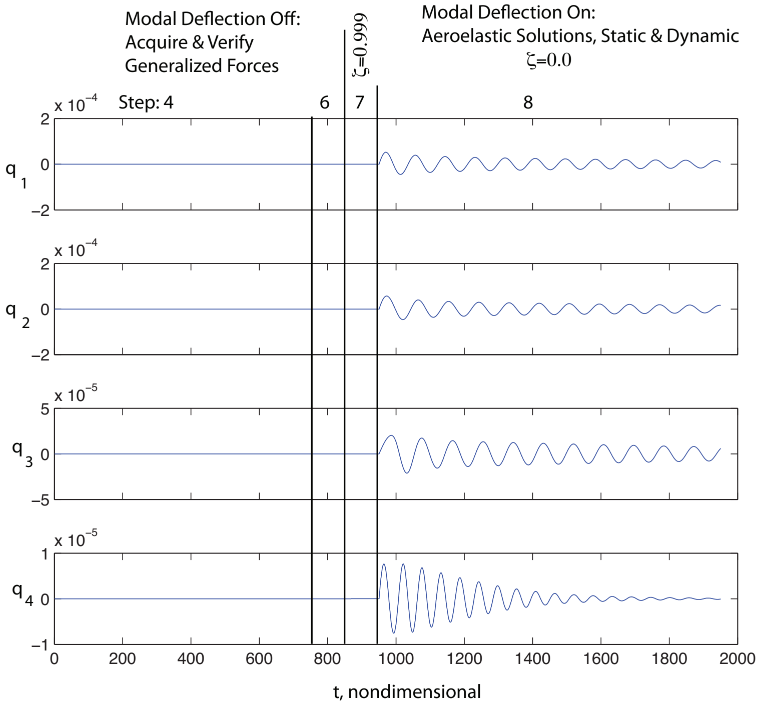

(b) Generalized coordinate time histories.

Figure 12. Generalized force and coordinate time histories for Mach 1.10, thin boundary layer, for a stable value of dynamic pressure, $q_\infty = 5.5 q_\infty^{nominal}$. The dynamic analysis was preceded by a converged nonlinear static aeroelastic solution.

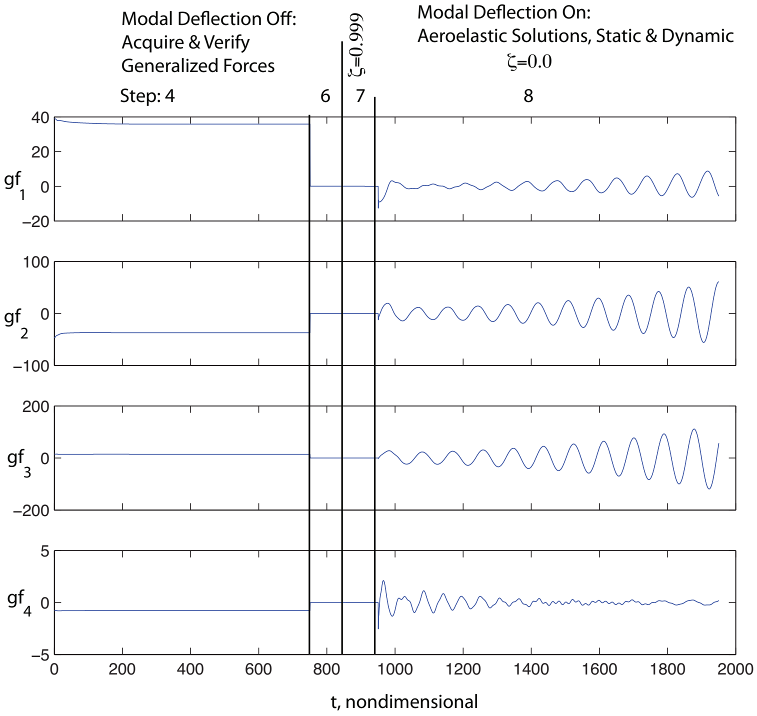

(a) Generalized force time histories.

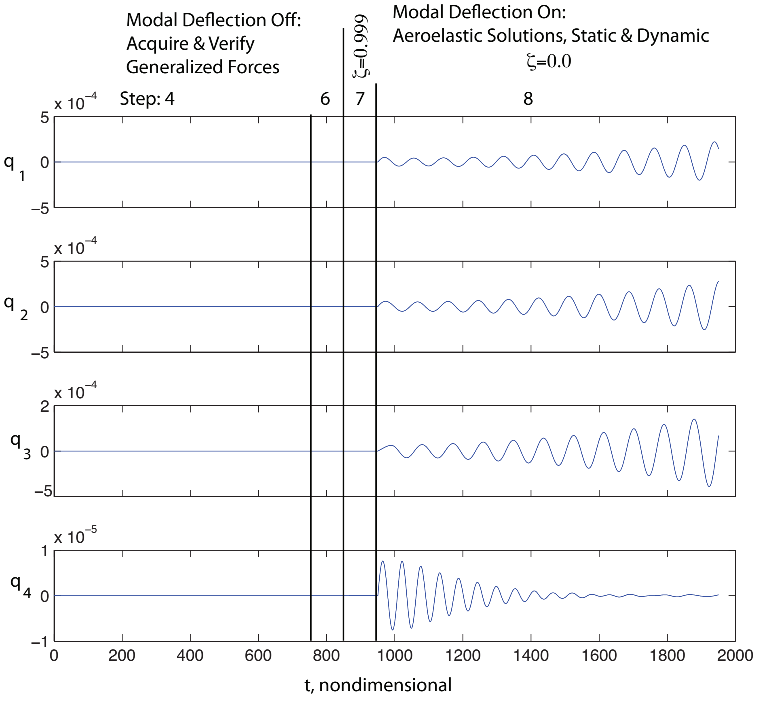

(b) Generalized coordinate time histories.

Figure 13. Generalized force and coordinate time histories for Mach 1.10, thin boundary layer, for an unstable value of dynamic pressure, $q_\infty = 6.5 q_\infty^{nominal}$. This dynamic analysis was preceded by a converged nonlinear static aeroelastic solution. Flutter frequency = 143 Hz.

are also labeled above. Step 4 is where the generalized forces are allowed to converge to nonzero values as shown in Figure 12(a). After the converged values of generalized force are added to the CFL3D input deck, the generalized forces all have a value of zero for steps 6 and 7. Finally, in step 8 modal deflection is turned on and the generalized forces change dynamically with the generalized coordinates shown in Figure 12(b). For this analysis, the panel is aeroelastically stable.

This analysis was repeated for $q_\infty = 6.5q_\infty^{nominal}$ with the time histories shown in Figure 13. Here, the panel is clearly unstable with a flutter frequency of 143 Hz which is consistent with the normal mode frequencies for modes 1 and 2 shown in Figure 9 for 0.1 psi pressure difference. In this instance, the inclusion of static nonlinear effects was a stabilizing effect.

# 5 Concluding Remarks

An on-orbit installable Space Shuttle overlay panel was developed at the NASA Johnson Space Center to be used in the event of damage to the thermal protection system tiles to enable safe re-entry. Previous flutter analyses indicated that at Mach numbers of 2.0 and higher, adequate panel flutter margins existed within the shuttle flight envelope. However, near Mach 1.0 empirical flutter analysis yielded inadequate flutter margins. As a result, CFD flutter analyses were conducted indicating that when viscous effects were considered, adequate flutter margins existed.

The present study has expanded on the previous work by looking in more detail at the effects of boundary layer thickness for additional Mach numbers near sonic speeds. In addition, the effects of structural damping were considered, as well as, structural nonlinearities associated with in-plane forces in the panel. These analyses described in this report indicated that the Space Shuttle overlay panel has adequate flutter margins for Mach numbers of 2.0 and below. The analysis showing the lowest, yet still adequate, flutter margin was the Mach 1.1, thin boundary case. More detailed conclusions are listed below.

- The results of the present study are consistent with those of reference 3.
- Flutter onset is relatively insensitive to boundary layer thickness near Mach 2.0, but thicker boundary layers have a stabilizing effect near sonic speeds.
- As expected, the addition of structural damping tended to increase the flutter onset dynamic pressure for the overlay panel. In addition, the results suggest that damping is more effective at stabilizing the panel at near sonic Mach numbers than at supersonic Mach numbers. A more detailed analysis would be required to confirm and quantify this trend.
- The nonlinear structural effects of a static pressure difference across the panel was examined. It was shown that a pressure differential results in increased stiffness and modal frequencies.
- A procedure for performing a static aeroelastic analysis with nonlinear structural effects followed by a dynamic aeroelastic analysis within CFL3D was described and demonstrated. For the case examined, the static pressure difference and the inclusion of static nonlinear structural effects resulted in a significant increase in flutter margin.

# References

1. Lemley, C. E.: Design Criteria for the Prediction and Prevention of Panel Flutter, Volume I: Criteria Presentation. AFFDL-TR 67-140, 1967.

2. Krist, S. L.; Biedron, R. T.; and Rumsey, C. L.: CFL3D User's Manual (Version 5.0). NASA/TM-1998-208444, June 1998.

3. Bey, K. S.; Scott, R. C.; Bartels, R. E.; Waters, W. A.; and Chen, R.: Flutter Analysis of the Shuttle Tile Overlay Repair Concept. NASA/TM-2007-214857, Mar. 2007.

4. Buning, P. G.; Jespersen, D. C.; Pulliam, T. H.; Klopfer, G. H.; W. M. Chan, J. P. S.; Krist, S. E.; and Renze, K. J.: OVERFLOW User's Manual, Version 1.8m. , Jan. 2000.

5. Cuneo, J.: A-Basis Mechanical Thermal Properties of GE 2D C/CSiC for RCC Plug Program. ITAR Test Report SRI-ENG-06-15-11502.01, Huntsville, AL, 2006.

6. MSC.Nastran 2005. Installation and operations guide, 815 Colorado Blvd., Los Angeles, CA 90041, 2005.

7. Bartels, R. E.: CFL3D Version 6.4 General Usage and Aeroelastic Analysis. NASA/TM-2006-214301, 2006.

8. Bertin, J. J.: *Engineering Fluid Mechanics*. Prentice-Hall, Inc., 1984.

9. Samareh, J. A.; and Bhatia, K. G.: A Unified Approach to Modeling Multidisciplinary Interactions. *AIAA/NASA/USAF/ISSMO Multidisciplinary Analysis and Optimization Symposium*, no. 2000-4704, Long Beach, California, Sept. 2000.

10. Smalley, K. B.; Tinker, M. L.; and Fischer, R. T.: Investigation of Nonlinear Pressurization and Modal Restart in MSC/NASTRAN for Modeling Thin Film Inflatable Structures. *42nd AIAA/ASME/ASCE/AHS/ASC Structures, Structural Dynamics, and Materials Conference and Exhibit*, no. 2001-1409, Apr. 2001.

11. Scott, R. C.; E.Bartels, R.; and Kandil, O. A.: An Aeroelastic Analysis of a Thin Flexible Membrane. *48th AIAA/ASME/ASCE/AHS/ASC Structures, Structural Dynamics, and Materials Conference*, no. 2007-2316, Honolulu, Hawaii, Apr. 2007.

12. MATLAB. Users guide, 3 Apple Hill Drive, Natick, MA 01760, 2008.

| | |
|---|---|
| **REPORT DOCUMENTATION PAGE** | *Form Approved*<br>*OMB No. 0704-0188* |

The public reporting burden for this collection of information is estimated to average 1 hour per response, including the time for reviewing instructions, searching existing data sources, gathering and maintaining the data needed, and completing and reviewing the collection of information. Send comments regarding this burden estimate or any other aspect of this collection of information, including suggestions for reducing this burden, to Department of Defense, Washington Headquarters Services, Directorate for Information Operations and Reports (0704-0188), 1215 Jefferson Davis Highway, Suite 1204, Arlington, VA 22202-4302. Respondents should be aware that notwithstanding any other provision of law, no person shall be subject to any penalty for failing to comply with a collection of information if it does not display a currently valid OMB control number.
**PLEASE DO NOT RETURN YOUR FORM TO THE ABOVE ADDRESS.**

| | | |
|---|---|---|
| **1. REPORT DATE** *(DD-MM-YYYY)*<br>01- 04 - 2009 | **2. REPORT TYPE**<br>Technical Memorandum | **3. DATES COVERED** *(From - To)* |

| | |
|---|---|
| **4. TITLE AND SUBTITLE**<br>Flutter Sensitivity to Boundary Layer Thickness, Structural Damping, and Static Pressure Differential for a Shuttle Tile Overlay Repair Concept | **5a. CONTRACT NUMBER** |
| | **5b. GRANT NUMBER** |
| | **5c. PROGRAM ELEMENT NUMBER** |
| **6. AUTHOR(S)**<br>Scott, Robert C.; Bartels, Robert E. | **5d. PROJECT NUMBER** |
| | **5e. TASK NUMBER** |
| | **5f. WORK UNIT NUMBER**<br>377816.06.02.03.20 |
| **7. PERFORMING ORGANIZATION NAME(S) AND ADDRESS(ES)**<br>NASA Langley Research Center<br>Hampton, VA 23681-2199 | **8. PERFORMING ORGANIZATION REPORT NUMBER**<br>L-19552 |
| **9. SPONSORING/MONITORING AGENCY NAME(S) AND ADDRESS(ES)**<br>National Aeronautics and Space Administration<br>Washington, DC 20546-0001 | **10. SPONSOR/MONITOR'S ACRONYM(S)**<br>NASA |
| | **11. SPONSOR/MONITOR'S REPORT NUMBER(S)**<br>NASA/TM-2009-215708 |

**12. DISTRIBUTION/AVAILABILITY STATEMENT**
Unclassified - Unlimited
Subject Category 02
Availability: NASA CASI (443) 757-5802

**13. SUPPLEMENTARY NOTES**

**14. ABSTRACT**

This paper examines the aeroelastic stability of an on-orbit installable Space Shuttle patch panel. CFD flutter solutions were obtained for thick and thin boundary layers at a free stream Mach number of 2.0 and several Mach numbers near sonic speed. The effect of structural damping on these flutter solutions was also examined, and the effect of structural nonlinearities associated with in-plane forces in the panel was considered on the worst case linear flutter solution. The results of the study indicated that adequate flutter margins exist for the panel at the Mach numbers examined. The addition of structural damping improved flutter margins as did the inclusion of nonlinear effects associated with a static pressure difference across the panel.

**15. SUBJECT TERMS**
Aerodynamics; Boundary layer; Flutter; Flutter sensitivity; Shuttle tile

| **16. SECURITY CLASSIFICATION OF:** | | | **17. LIMITATION OF ABSTRACT** | **18. NUMBER OF PAGES** | **19a. NAME OF RESPONSIBLE PERSON** |
|---|---|---|---|---|---|
| **a. REPORT** | **b. ABSTRACT** | **c. THIS PAGE** | | | STI Help Desk (email: help@sti.nasa.gov) |
| | | | | | **19b. TELEPHONE NUMBER** ***(Include area code)*** |
| U | U | U | UU | 30 | (443) 757-5802 |